http://www.zju.edu.cn/jzus; E-mail: jzus@zju.edu.cn
ISSN 1009-3095 *Journal of Zhejiang University SCIENCE* V.4, No.6, P.683-693, Nov.-Dec., 2003

Study on pile drivability with one dimensional wave propagation theory*

CHEN Ren-peng(陈仁朋)†1, WANG Shi-fang(王仕方)2, CHEN Yun-min(陈云敏)1
(1 *Geotechnical Engineering Institute, Dept. of Civil Engineering, Zhejiang University, Hangzhou 310027, China*)
(2 *Wenling Construction Bureau, Wenling 317500, Zhejiang Province, China*)
†E-mail: crp@civil.zju.edu.cn

Received Oct.8, 2002; revision accepted May 5, 2003

Abstract: Pile drivability is a key problem during the stage of design and construction installation of pile foundations. The solution to the one dimensional wave equation was used to determine the impact force at the top of a concrete pile for a given ram mass, cushion stiffness, and pile impedance. The kinematic equation of pile toe was established and solved based on wave equation theory. The movements of the pile top and pile toe were presented, which clearly showed the dynamic displacement, including rebound and penetration of pile top and toe. A parametric study was made with a full range of practical values of ram weight, cushion stiffness, dropheight, and pile impedance. Suggestions for optimizing the parameters were also presented. Comparisons between the results obtained by the present solution and in-situ measurements indicated the reliability and validity of the method.

Key words: Pile, Drivability, Stress-wave theory
Document code: **CLC number:** TU473

INTRODUCTION

Interest in one dimensional wave propagation theory for application to understanding pile driving is more than a century old. Important work directly related to current applications to pile drivability started shortly after the Second World War and continued to the present, as such problem is not only the concern of the contractor but also of the investor. Probably the most remarkable work in developing quantitative solutions was done by Smith (1960), whose program of the so-called "Wave Equation" could possible be the first application of electronic digital computers to a civil engineering problem. With the discreted pile driving model, the program could provide the driving resistance, pile movement, impact force and so on. After the invonvative work of Smith (1960) and Rausche *et al.* (1972, 1985) developed a method to estimate the pile capacity and pile integrity. Today, although the GRLWEAP™ program is widely used in the United States, its usage outside the U.S. is much less common (Goble, 2000). Except for the discereted method, some formulas similar to the pile driving formulas, based on the one dimensional wave propagation theory, were developed to manage pile driving (Uto *et al.*, 1992; Weele and Schellingerhout, 1994; Chen *et al.*, 1997). Chen *et al.* (2000, 2001b) explored the relationship between rebound of the pile top and the driving resistance.

It is difficult to calculate accurately the pile hammer interaction when considering simplified systems and employing wave propagation theory (Rausche, 2000). Therefore it is best to measure the force and the velocity at the pile top and calculate the desired quantities based on the measurement. At the beginning of construction, such in-situ measurement cannot be carried out, and prediction is necessary to select the optimal parameters of piles, installation and return on investment.

Clough and Penzien (1975) first obtained the impact force on the pile top when the free drop hammer impacts on the elastic pile top, this approach is also employed in this paper. The one dimensional wave propagation theory was used to establish and solve the kinematic

* Project (No.50278087) supported by the National Natural Science Foundation of China

equation for the pile toe. The movements of the pile toe and the pile top are presented clearly indicating the rebound and penetration of the pile. The influences of the parameters of the driving system and of the pile impedance, on the pile drivability were discussed.

PILE DRIVING MODEL

Impact force

The pile driving process can be separted into two stages: (a) the interaction of pile and hammer, and (b) the penetration of the pile into the ground after it is impacted by the hammer. It is impossible to set up an accurate model for the interaction of pile and hammer because of the complexity of the driving equipment. Clough and Penzien (1975) solved the problem shown in Fig.1 (a). The pile driving system is modeled

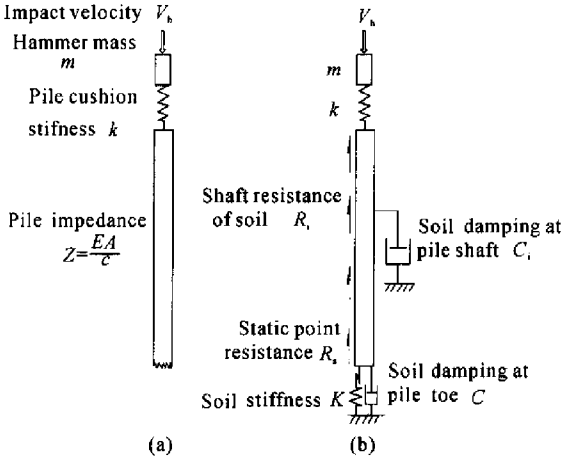

Fig.1 Pile driving model

(a) model used by Clough and Penzien (1975)
(b) model used in this paper

by three elements: a rigid ram, a linear spring (pile cushion) and an elastic pile. The solution yields the delivered impact force induced at the pile top during the first wave passage, as expressed in Eq. (1)

$$F(t) = \frac{kV_h}{\omega_d} e^{-\xi\omega t} \sin\omega_d t, \quad 0 \leqslant \omega_d t \leqslant \pi \tag{1}$$

where $\omega^2 = k/m$, $\omega_d = \omega\sqrt{1-\xi^2}$, $\xi = kc/(2\omega EA)$. k, m, E and A are defined in Fig.1 (a), and c is wave velocity. V_h is ram impact velocity, a very important factor, obtained from the kinetic hammer energy (E_t) mentioned by hammer manufacturers,

$$V_h = \sqrt{2eE_t/m} \tag{2}$$

where e is the hammer efficiency, which is the ratio of kinetic energy available to do work on the driving system, the pile and soil, to potential energy, and g is the gravity acceleration, $9.8 m/s^2$. The hammer efficiency e describes the percentage of maximum hammer energy transferred to the pile and soil, and is a very important quantity that defines the ability of a hammer to move the pile into the ground. The energy losses due to friction, misalignment, low stroke and pre-ignition are different for different types of hammer. Table 1 shows the typical hammer efficiency e of several types of hammers. Table 2 shows the dynamic hammer data after Lucieer (2000).

Eq.(1) shows that the shape of the impact force is similar to that of a half sinusoid. There are three characteristic parameters describing the shape: the peak impact force F_0, duration t_0 and loading period t_1,

$$F_0 = \frac{kV_h}{\omega_d} e^{-\xi\omega t_1} \sin\omega_d t_1$$

$$t_0 = \frac{\pi}{\omega_d}$$

$$t_1 = \frac{1}{\omega_d} \arctan\frac{\omega_d}{\omega\zeta}$$

Eq.(1) is rather difficult to be used in analytical study. Then the impact is simplified as

Table 1 Hammer efficiency of different type of hammers

Hammer type	Free release drop hammer	Single acting air/steam hammer	Diesel hammer	Hydraulic drop hammer	Self-monitored hydraulic hammer
Hammer efficiency	0.95	0.67	0.8	0.9	0.95

Table 2 Dynamic hammer data (after Lucieer, 2000)

Type remarks*	Mass of ram (ton)	Impedance of hammer (MNs/m)	Impact velocity V_h (M/s)	Hammer types
IHC-S70	4.5	7.0	6.3	Hydraulic
DELMAG-100	10	10.6	4.5	Diesel
MRBS3000	30	40.9	4.7	Steam

* Remarks give the process of lifting the ram. The ram of the IHC-S70 hammer is pushed down, resulting in a smaller stroke of the ram. The ram MRBS3000 is free falling. The fall of the piston of the diesel hammer Delmag D-100 is slowed down by the compressed gas

$$F(t) = F_0 \begin{cases} \dfrac{t}{t_1} & 0 \leqslant t < t_1 \\ \dfrac{t_0 - t}{t_0 - t_1} & t_1 < t \leqslant t_0 \end{cases} \tag{3}$$

Comparison between Eqs. (1) and (3) is depicted in Fig.2, showing the similarity of the two patterns of force.

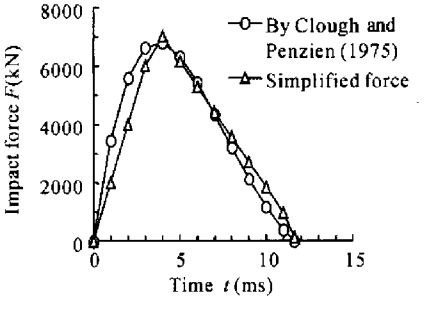

Fig.2 Impact force calculated by Eq.(1) and the simplified triangular force

Pile toe movement

Wave Equation analysis is now used routinely in pile driving practice. The model used for Wave Equation analysis is shown in Fig.1(b). Soil at the pile shaft is postulated to be rigid-plastic, and soil at the pile toe is postulated to be elastoplastic and described by Smith Soil Model (Smith, 1960). No residual compression of piles during driving is taken into account. Considering the continuity of force at the pile toe, the kinematic equation of the pile toe can be described as in Chen *et al*. (2001a; 2001b)

$$(C + Z)V(t) + K[U(t) - U_p(t)] = 2F_d(t) \tag{4}$$

where $U(t)$ and $V(t)$ are the movement and velocity of the pile toe respectively, and $U_p(t)$ is the penetration of the pile toe; $F_d(t)$ is the downward force, which is equal to the impact force at the pile top $F(t)$ subtracted by the motivated shaft resistance $R_d(t)$ while the stress-wave propagates downward. The motivated shaft resistance is written as

$$R_d(t) = \begin{cases} \dfrac{F_0 C_i t}{2Zt_1} + \dfrac{R_i}{2} & 0 \leqslant t < t_1 \\ \dfrac{F_0 C_i (t - t_0)}{2Z(t_1 - t_0)} + \dfrac{R_i}{2} & t_1 < t \leqslant t_0 \end{cases} \tag{5}$$

The movement of the pile toe (or soil at the pile toe) can be divided into three stages: elastic movement, penetration and rebound (Chen and Chen, 2000). When the movement of the pile toe is less than the maximum elastic deformation, known as quake Q_p, there is only elastic deformation. The static soil resistance increases linearly with the movement of the pile toe until it reaches the maximum static resistance R_s. When the movement of the pile toe exceeds quake, the pile toe penetrates into the soil and the static soil resistance remains constant. When the movement of the pile toe reaches to its limit, then rebound occurs and the static soil resistance decreases from R_s. Fig.3 is used to model the soil behavior during the above three stages of the pile toe movement.

The following seven dimensionless parameters are introduced

$$n = R_s/F_0;\ n_i = R_i/F_0;\ \eta = t_1/t_0;\ \lambda = R_i/R_s;$$
$$m_1 = Z/(Kt_0);\ m_2 = C/(Kt_0);\ m_{2i} = C_i/(Kt_0)$$

With the assumption of Smith damping law, with

$$m_1 = \frac{Q_p}{nV^t_{max}t_0},\quad m_2 = \frac{Q_p J_p}{t_0},$$
$$m_{2i} = \frac{\lambda Q_p J_s}{t_0}$$

where J_p and J_s are the Smith damping coefficients of the soil at the pile toe and around the

pile shaft, respectively. Solving the combination of Eqs. (3), (4) and (5) yields the dimensionless form of the movement and the velocity at the pile toe as

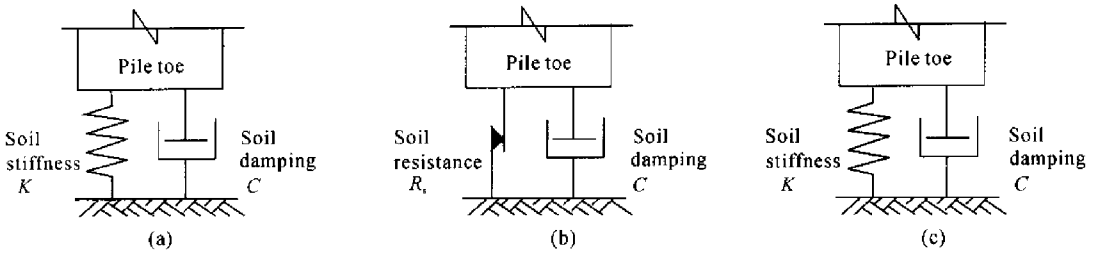

Fig.3 Models of pile toe in different stages

(a) model for elastic movement; (b) model for plastic deformation; (c) model for rebound

$$\frac{K}{F_0}U(\tau)=\begin{cases}\dfrac{2}{\eta}\tau-n_i-\dfrac{2m}{\eta}-\dfrac{m_{2i}}{m_1\eta}(\tau-m)+\left(n_i+\dfrac{2m}{\eta}-\dfrac{mm_{2i}}{m_1\eta}\right)e^{-\frac{\tau}{m}} & 0\leqslant\tau<\eta\\ \dfrac{2(\tau-1)}{(\eta-1)}-n_i-\dfrac{2m}{(\eta-1)}-\dfrac{m_{2i}}{m_1(\eta-1)}(\tau-m-1)+ & \\ \quad\left[\left(n_i+\dfrac{2m}{\eta}-\dfrac{mm_{2i}}{m_1\eta}\right)e^{-\frac{\eta}{m}}+\dfrac{m}{\eta(\eta-1)}\left(2-\dfrac{m_{2i}}{m_1}\right)\right]e^{-\frac{(\tau-\eta)}{m}} & \eta\leqslant\tau<\tau_p\\ \dfrac{(\tau-1)^2}{m(\eta-1)}-\dfrac{(n+n_i)}{m}\tau-\dfrac{m_{2i}(\tau-1)^2}{2mm_1(\eta-1)}+w_1 & \tau_p\leqslant\tau\leqslant\tau_r\\ \dfrac{2(\tau-1)}{(\eta-1)}-n_i+\dfrac{K}{F_0}S-\dfrac{2m}{(\eta-1)}-\dfrac{m_{2i}}{m_1(\eta-1)}(\tau-m-1)+ & \\ \quad w_2e^{-\frac{\tau}{m}} & \tau_r\leqslant\tau<1\\ \dfrac{K}{F_0}S+w_3e^{-\frac{\tau}{m}} & 1\leqslant\tau\end{cases}\tag{6}$$

$$\frac{Kt_0}{F_0}V(\tau)=\begin{cases}\dfrac{2}{\eta}-\dfrac{m_{2i}}{m_1\eta}-\left(\dfrac{n_i}{m}+\dfrac{2}{\eta}-\dfrac{m_{2i}}{m_1\eta}\right)e^{-\frac{\eta}{m}} & 0\leqslant\tau<\eta\\ \dfrac{2}{(\eta-1)}-\dfrac{m_{2i}}{m_1(\eta-1)}- & \\ \quad\left[\left(\dfrac{n_i}{m}+\dfrac{2}{\eta}-\dfrac{m_{2i}}{m_1\eta}\right)e^{-\frac{\eta}{m}}+\dfrac{(2m_1-m_{2i})}{m_1\eta(\eta-1)}\right]e^{-\frac{(\tau-\eta)}{m}} & \eta\leqslant\tau<\tau_p\\ \dfrac{2(\tau-1)}{m(\eta-1)}-\dfrac{(n+n_i)}{m}-\dfrac{m_{2i}(\tau-1)}{mm_1(\eta-1)} & \tau_p\leqslant\tau\leqslant\tau_r\\ \dfrac{2}{(\eta-1)}-\dfrac{m_{2i}}{m_1(\eta-1)}-\dfrac{w_2}{m}e^{-\frac{\tau}{m}} & \tau_r\leqslant\tau\leqslant1\\ -\dfrac{w_3}{m}e^{-\frac{\tau}{m}} & 1\leqslant\tau\end{cases}\tag{7}$$

where $m=m_1+m_2$, $\tau=t/t_0$, τ_r and τ_p are the dimensionless times when plastic movement and rebound take place respectively, w_1, w_2 and w_3 are integration constants, S is the total penetration of the pile toe. τ_r, τ_p, w_1-w_3 can be obtained by considering the continuity of the movement and velocity of the pile toe at each stage.

Movement of pile toe

The movement of the pile toe under each blow is described in Eq.(6). As residual compression in the pile was not considered, the movement of the pile top is assumed to be equal

to that of the pile toe. The typical movement of the pile top is depicted in Fig.4. The three stages of movement of the pile toe mentioned above can be clearly distinguished. When the impact force acts on the pile top, the pile toe immediately moves downward and the soil deforms linearly. With the increase of impact force, the pile toe moves downward rapidly and the plastic deformation of the soil occurs. Generally, it takes 1 to 2 ms from loading for soil to deform plastically. The rate of penetration decreases to zero when the impact force decays. This is the beginning of the rebound of the pile toe. Then the pile toe moves upward. The dynamic movement of the pile top recorded by the Optical Displacement System (Chen *et al.*, 1997) is depicted in Fig. 5. Compared to the measured movement of the pile top, the calculated movement of the pile top, Fig.4, is smoother, without considering the reflection of stress-wave at the pile top.

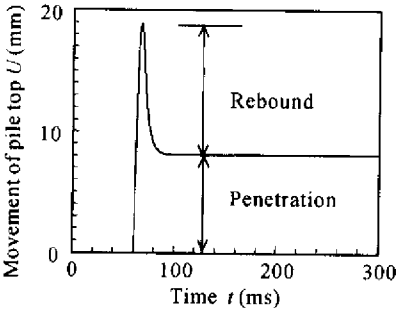

Fig.4 Movement of the pile top calculated by Eq.(6)

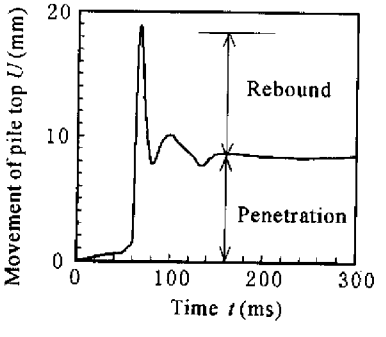

Fig.5 Movement of the pile top measured by Optical Displacement System (Chen *et al.*, 1997)

The penetration of the pile under each blow is expressed as

$$\frac{K}{F_0}S = \frac{(\tau_r - 1)^2}{m(\eta - 1)} - \frac{(n + n_i)}{m}\tau_r - \frac{m_{2i}(\tau_r - 1)^2}{2mm_1(\eta - 1)} + w_4 - \frac{2(\tau_r - 1)}{\eta - 1} + n_i + \frac{2m}{\eta - 1} + \frac{m_{2i}(\tau_r - m - 1)}{m_1(\eta - 1)} - w_2 e^{-\frac{\tau_r}{m}} \quad (8)$$

If no residual compression of the pile is taken into account, the rebound of the pile top is expressed by

$$R_e = U^t_{max} - U^b_{max} + Q_p \quad (9)$$

where U^t_{max} and U^b_{max} are the maximum displacements of the pile top and the pile toe respectively. $(U^t_{max} - U^b_{max})$ was obtained by Chen *et al.* (2000; 2001b), as follows

$$U^t_{max} - U^b_{max} = \alpha_1 \frac{R_s t_0}{Z} - \alpha_2 \frac{R_i t_0}{Z} \quad (10)$$

where $\alpha_1 = \frac{(1-\beta)}{2(2-m_{2i})}$; $\alpha_2 = -\alpha_1 + \frac{(T^2-\beta^2)}{4T} + \frac{\beta}{2} + \frac{m_{2i}(1-\beta)^2}{2m_1 n_i(1-\eta)}$; $T = 2L/c$; and β is the time when the actual velocity of the upward wave reaches zero.

Substituting Eq.(10) into Eq.(9) yeilds the rebound of the pile top as

$$R_e = \frac{R_s t_0}{Z}\frac{1 - \lambda C_d}{C_s} \quad (11)$$

where $C_s = (\alpha_1 + m_1)^{-1}$, $C_d = \alpha_2(\alpha_1 + m_1)^{-1}$.

In-situ measurement showed that C_s and C_d varied little, with C_s being equal to 1.3, and C_d being equal to 0.7 (Chen *et al.*, 2001b). It can be seen that the rebound is greatly influenced by the point resistance. The greater the point resistance is, the larger the rebound will be. But the shaft resistance has a negative effect on the rebound. The greater the shaft resistance is, the less the rebound will be. Such phenomenon has been proved in practice. During hard driving (for example, the pile toe reaches a very stiff soil layer), the pile rebounds strongly. After the connection of different segments, the set up of pile increases the shaft resistance, leading to decreased rebound of the pile.

DETERMINATION OF SOIL RESISTANCE

Rewriting Eq.(11), the expression of R_s

can be expressed as follows

$$R_s = \frac{C_s}{(1-\lambda C_d)} \frac{R_e Z}{t_0} \qquad (12)$$

With Eq.(12), it is easy to estimate the point resistance. Such technique was reported by Chen *et al*.(1997), de Albuquerque and de Carvalho (2000) and Uto *et al*. (1992). de Albuquerque and de Carvalho (2000) introduced a new type of sensor, called reboundmeter, to measure the displacement of the pile top. By integrating the measured acceleration of the pile top with a special technique, Chen *et al*. (1997) obtained with acceptable accuracy the velocity and displacement of the pile top. The rebound (R_e) and impact duration (t_0) are determined from the movement of the pile top. Then the curve of static point resistance vs pile toe depth during the pile driving is simultaneously obtained, as shown in Fig.6.

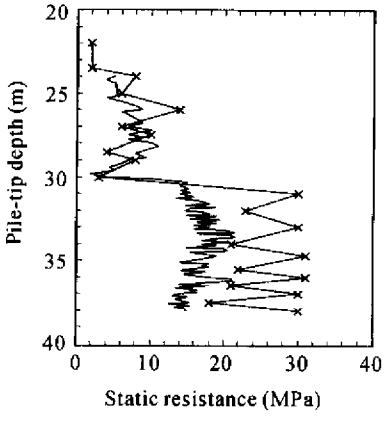

Fig.6 Cone resistance of CPT and the point resistance estimated by Eq.(12)

* Cone resistance of CPT;
– Static point resistance estimated by Chen *et al*.(1997)

The structure of the estimated point resistance is similar to that of the cone resistance of CPT (Cone Penetration Test). Because of the influence of the size effect, the point resistance of the pile toe is much less than that of CPT.

PILE DRIVABILITY

Pile drivability is no doubt most serious concerned to civil engineers and is very difficult to predict, because of the complicated properties of the driving machine, different geological conditions and the pile. For a certain construction site, engineers always try to answer the following questions: (1) how to select length, diameter and material of pile, and (2) how to select the driving machine and the type of hammer, cushion, and so on.

Hammer mass and dropheight

The influence of hammer mass and dropheight on the impact peak force, impact duration and pile penetration are shown in Figs.7, 8 and 9, respectively. The greater the mass of the hammer is, the greater the impact peak force and the longer the impact duration. A large hammer has

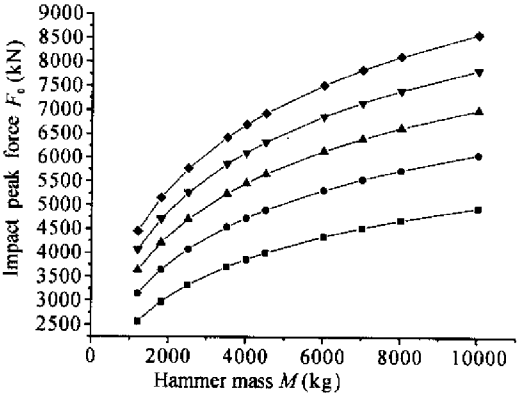

Fig.7 Influence of hammer mass and dropheight on impact peak force

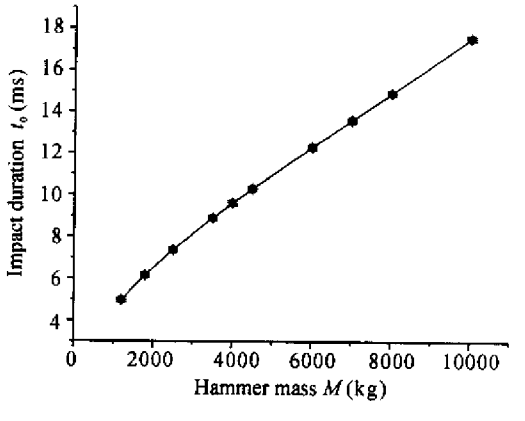

Fig.8 Influence of hammer mass and dropheight on impact duration

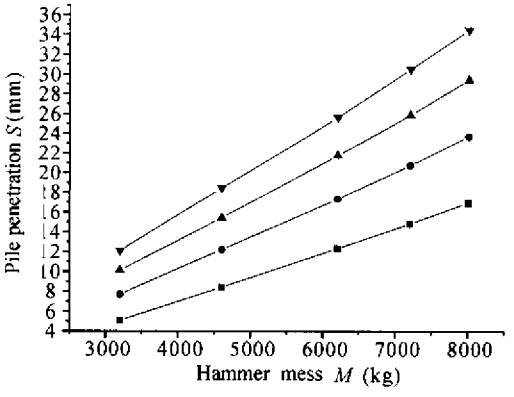

Fig.9 Influence of hammer mass and dropheight on penetration

—■— h=1000 mm —●— h=1500 mm —▲— h=2000 mm —▼— h=2500 mm

the ability to maintain the pile top force near the maximum impact force. Therefore, a small hammer will only generate a short force pulse, which may be ineffective in maintaining a sustained downward movement and pile penetration. As the maximum force in the pile at the beginning of the impact event is primarily dependent on the impact velocity, so a greater dropheight can also generate a greater peak force like that of a larger hammer. However, it is impossible to extend the maximum force, i.e. impact duration by increasing the dropheight. Greater impact force is the main reason for the destruction of the pile top during continuous driving. On the other hand, a slowly falling hammer cannot generate the necessary force to overcome the soil resistance.

The most advisable peak force should have the ability to overcome the soil resistance but not destroy the pile top. To achieve deeper penetration, longer impact duration is better. In other words, the impact force should be generated by a large hammer with a low dropheight, not a small hammer with a high dropheight.

Pile cushion

A set of driving system includes a cushion for the protection of the hammer, a helmet with adaptors and a cushion to protect concrete piles. Many diesel hammer manufacturers do not make hammer cushion driving system with the confidence of making well fitting and machined impact surface for the ram so that high contact stresses are avoided. The helmet is used to align hammer and pile and uniformly spread the impact force over the pile top. Pile cushions are necessary for concrete piles where they serve two purposes. Firstly they must reduce the likelihood of stress concentrations at points of steel-concrete contact. Secondly they are often designed to reduce the peak stress in the pile by spreading the impact forces over time. Pile cushions are made of a variety of materials, including straw, plywood, hamortex, and other kinds of man-made material. Pile cushions made of straw and plywood, only last for about 1500 hammer blows. This limit can be a problem for driving for an extended time period. Figs. 10 – 12 show the influence of stiffness of pile cushions on peak force, impact duration and pile penetration respectively. When the pile cushion gets stiffer and stiffer the peak force increases rapidly and the impact duration decreases rapidly. During pile driving, the pile cushion becomes stiffer with the continuous blows. The train of excessive peak force and short impact duration decreases the driving eff-

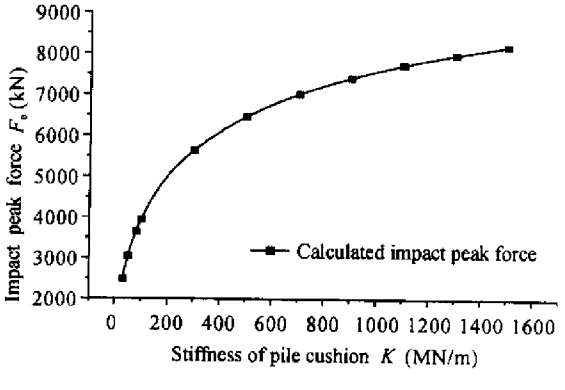

Fig.10 Influence of pile cushion on peak force

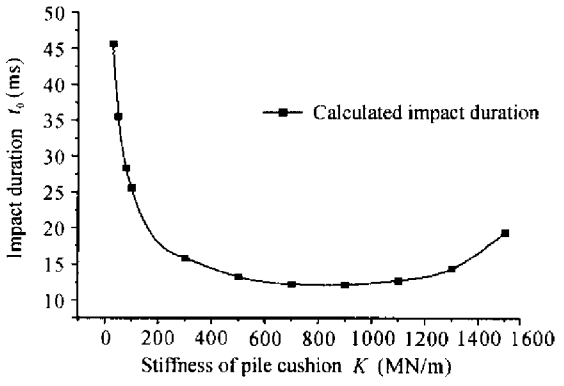

Fig.11 Influence of pile cushion on impact duration

iciency and increases the possibility of damage of pile material. It is shown distinctly in Figs. 10 – 12 that when the stiffness of the pile cushion is range from 150 to 500 MN/m, the penetration increases very little. There exists an optimal stiffness of pile cushion (in Fig. 12, it is about 100 MN/m.), for which the penetration will be much greater. Too soft cushion is not acceptable for low peak force and the consequently low penetration. Too stiff cushion is also not acceptable for high peak force with resulting possibility of pile damage. Adjusting the stiffness of the pile cushion may result in optimal driving efficiency.

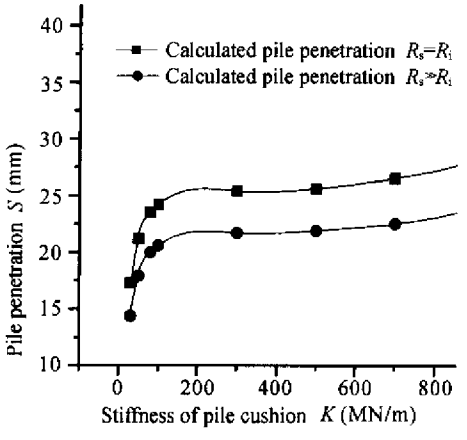

Parameters used in Figs. 10,11, and 12:
Hammer mass: 6.2 Mg
Dropheight: 2.5 m
Pile size: outer diameter 600 mm, thickness 110 mm
Pile density: 2400 kg/m^3
Concrete strength of pile: 50.5 MPa
Young modulus of pile: 38 GPa
Static point resistance: 1000 kN
Total shaft resistance: 1000 kN
Soil quake at pile toe: 2.54 kN
Soil damping at pile toe: J_p=0.48
Soil damping at pile shaft: J_s=0.16

Fig.12 Influence of pile cushion on penetration

Pile impedance

It was found that increase of pile impedance led to increase of peak force, and shortening of impact duration. Excessive number of hammer blows and compressive stress will cause pile damage and fatigue. Very briefly, the total number of hammer blow should be less than 2000 for concrete pile and 3000 for steel piles. For friction pile, blow counts should be less than 80 blows for 0.25 m. For end bearing piles, it is limited to 200 blows for 0.25 m because of the relatively short duration. According to Rausche (2000), compressive concrete stress should be less than 85% of the concrete strength. Tensile stress should amount to less than 70% of the equivalent yield strength of regular reinforcement of prestress concrete plus 50% of the concrete tensile strength. For steel pile, stresses should be less than 90% of the yield strength. The concrete strength increases with the rate of loading. The normal rate of loading in laboratory test is 0.15 to 0.2 MPa per second. If the rate of loading is increased to 10 MPa per second, the strength will increase 10% percent. And if the rate of loading is increased to 105 MPa per second, the strength will increase 60%. The general rate of loading during pile driving is about 104 MPa per second, so the dynamic concrete strength should be larger than the static concrete strength by up to 40% – 50%. Unfortunately, until now, there is no laboratory test to prove it, while in-situ monitoring always finds excessive concrete stress over the static concrete strength without damage of pile. Considering the fatigue of concrete, the concrete stress should be limited to a certain percentage of the dynamic strength. For the safety of the installation, the concrete stress should be less than the static concrete strength.

CASE HISTORY

Prestressed tube piles with outer diameter of 550 mm, thickness of 100 mm and length of approximately 51 m were used in a high building project. The pile toe was designed to penetrate into the 2 meters bearing stratum gravelly soil. The penetration for the last 10 blows should be less than 10 cm. A DELMAG diesel hammer, with mass of 8 Mg was selected to drive the piles. The contractor required drivability analysis beforehand to check the efficiency of the driving equipment and predict the drivability. The soil investigation included soil sampling and dynamic penetration test (DPT). The soil investigation showed that the soil consisted of muck, mucky soil, sandy soil, gravelly soil, and clay, properties as listed in Table 3. The soil profile is depicted in Fig. 13. The groundwater table lies approximately 2.0 m below ground level.

Table 3 Main soil properties

Soil No.	Soil type	Thickness of soil layers (m)	Water content (%)	Void ratio	Blow counts of DPT $N^{a}_{63.5}$	Static shaft resistance (MPa)	Static point resistance (MPa)
(2)	Muck	15.05	59.8	1.65	—	5	
(3-1)	Gravelly soil	1.75	—	—	8.7	30	
(3-2)	Mucky soil	10.65	47.3	1.27	—	10	
(4-1)	Gravelly soil	2.40	—	—	14	35	
(4-2)	Silty clay	10.25	31.7	0.94	—	22	
(5-1)	Gravelly soil	4.70	—	—	18.8	45	3000
(5-2)	Clay	2.00	34.6	0.94	—	30	1200
(6-1)	Sandy soil	6.30	43.1	1.16	—	20	700
(7-2)	Gravelly soil	>5.00	—	—	31	78	4000

Note: [a] $N_{63.5}$ means the blow counts to drive the cone into the soil for 10 cm, with a hammer of 63.5 kg

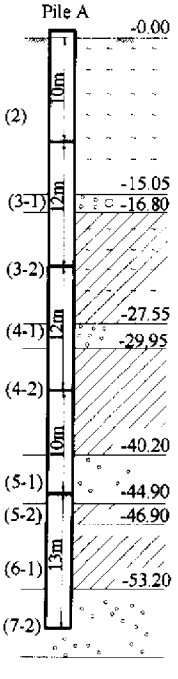

Fig.13 Soil profile at the location of Pile A

Analysis of drivability

Before construction, the drivability of three piles located at different places (Pile A to C) was analyzed. The total blow numbers for the three piles at different depth of pile toe are depicted in Fig. 14. The number of hammer blows per meter for the three piles are shown in Fig. 15. The total number of blows for Pile C, 1100 blows, was less than that for Pile A, 1580 blows, and Pile B, 1620 blows, because the ground level of the gravelly soil (7-2) at the location of Pile C was higher than that of Pile A and Pile B. The figures of blow number per meter vs. depth for the three piles vary little. At the depth of 40 meter (upper surface of the gravelly soil (5-1)), the blow counts decreased apparently, from 10 – 15 blows to 5 blows for 0.25 m. Accordingly, the penetration decreased from 5 cm to 1.7 – 2.5 cm per blow. After easily penetrating through the clay (5-2), the pile toe reacheed the sandy soil (6-1) layer at the 47 meter depth. When the pile toe was in this soil

layer, the blow count was 20 blows per meter, and the penetration was 1.3 cm per blow. It was not easy to drive through the gravelly soil (5-1) and sandy soil (6-1). When the pile toe reached the gravely soil (7-2), which was the designed bearing stratum, the blow counts increased rapidly and accordingly the penetration decreased rapidly. The blow number was only 27 – 42 blows per meter, and the penetration was 0.5 – 0.8 cm per blow. The peak force during driving was 7500 kN, with a corresponding concrete stress of 53 MPa being a little over the concrete strength of 50.5 MPa. Considering the influence of the loading rate on the concrete strength, the driving stress cannot damage the pile top. With the above analysis of drivability, it is deemed that the selected driving system could drive the pile to pass through the gravelly soil (5-1) and the sandy soil (6-1), and successfully penetrate the gravelly soil (7-2) to a designed depth. Table 4 shows of the measured and estimated results of blow counts. The estimated and measured blow counts vs. depth curves are depicted in Figs. 16, 17 and 18, showing that for depth greater than 40 m, the calculated blow count is almost twice or thrice the measured one. For the effect of set up, the blow count increases sharply at 48 meter depth where two segments are welded. The overestimated blow counts above 40 meter is mainly due to the simplification of the model. If the blow count caused by the set up during connection is excluded, the estimated blow count will agree well with the measured results.

The final bearing capacity of the three piles was obtained from the static load test with the load varying from 5000 to 6000 KN. Further integrity test showed the integrity of the three piles.

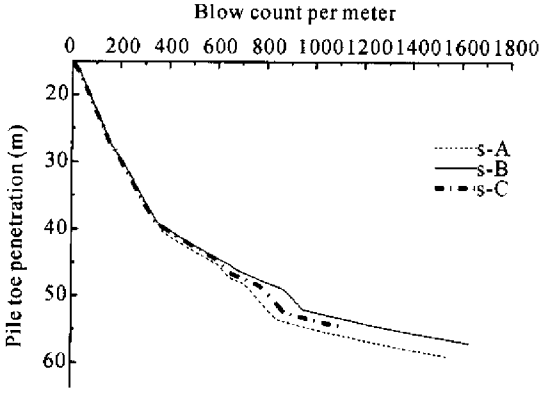

Fig.14 Total blow count vs depth

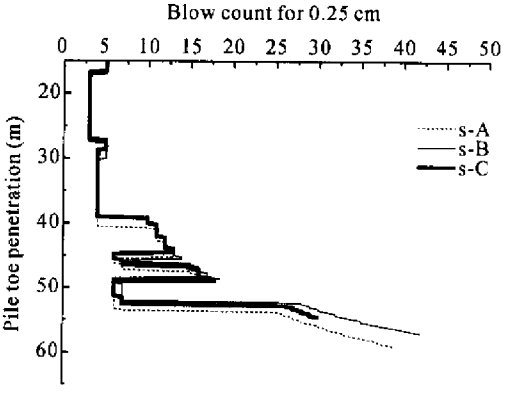

Fig.15 Estimated blow counts for 0.25 m vs depth for the three piles

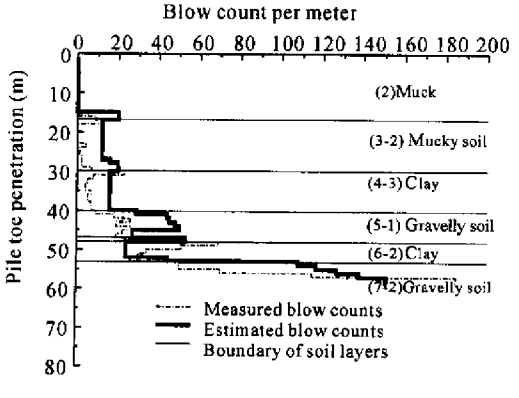

Fig.16 Measured blow count for 1 m vs depth for Pile A

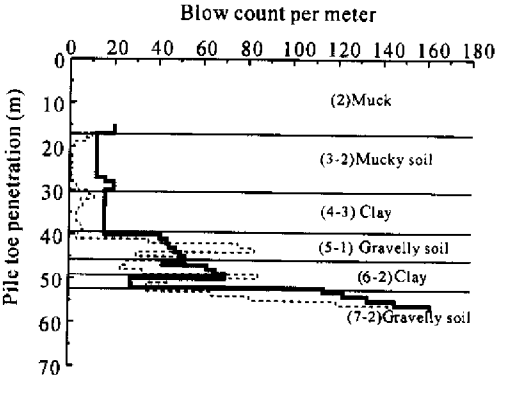

Fig.17 Measured blow count for 1 m vs depth for Pile B

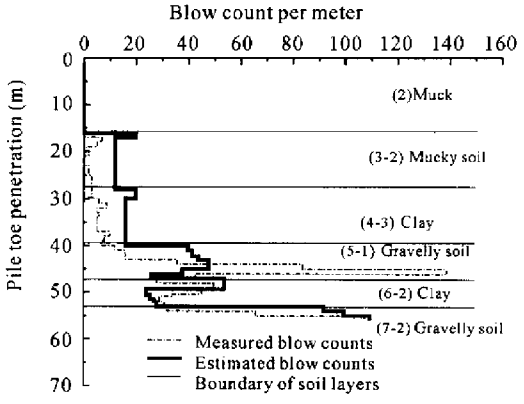

Fig.18 Measured blow counts for 1 m vs depth for Pile C

Table 4 Comparison of estimated and measured blow counts

Pile number	Blow counts for final 5 meters	Total blow counts	Blow counts for final 10 cm
Pile A	642/470	1580/960	16/18
Pile B	677/445	1620/1090	18/15
Pile C	301/275	1100/879	12/12

Note: 642/470 means estimated blow counts/measured blow counts

CONCLUSIONS

A theoretical analysis of pile drivability can be made and will lead to technical and economic success of a project. While many "rules of thumb" have been tried and dynamic formulas have been used to estimate the hammer size for a particular job, the wave equation theory is still the most reliable tool to determine the hammer size and driving system for reasonable blow counts and safe stress. The present technique helps to select the proper equipment, and to estimate the reasonable blow count, penetration, compressive stresses, and driving resistance for pile driving.

References

Chen, R. P. and Chen, Y. M., 2000. Theoretical Study on Effect of Pile Shaft Resistance on Rebound During Pile Driving. Proceedings of the 6th International Conference on the Application of Stress-wave Theory to Piles, Brazil, p. 29 – 34.

Chen, R. P., Chen, Y. M., Li, Q. and Tong, J. G., 2001a. Study of pile drivability with in-situ measurement. *Chinese Journal of Geotechnical Engineering*, **23**(2): 235 – 238 (in Chinese).

Chen, R. P., Hu, Y. Y. and Chen, Y. M., 2001b. Determine driving resistance with rebound of pile-top during pile driving. *Journal of Zhejiang University SCIENCE*, **2**(2): 179 – 185.

Chen, Y. M., Chen, R. P., Wu, S. M. and Van Weele, A. F., 1997. Determing static resistance of pile toe during driving with acceleration of pile top. *Chinese Journal of Geotechnical Engineering*, **19**(6): 16 – 21 (in Chinese).

Clough and Penzien, 1975. Dynamics of Structures. McGram-Hill, Inc., New York.

Goble, G. G., 2000. Some Wave Mechanics Applications, Proceedings of the 6th International Conference on the Application of Stress-wave Theory to Piles, Brazil, p. 3 – 9.

de Albuquerque, P. J. R. and de Carvalho, D., 2000. Dynamic Load Test and Elastic Rebound Analysis for Estimation of the Bearing Capacity of Piles in Residual Soil. Proceedings of the 6th International Conference on the Application of Stress-wave Theory to Piles, Brazil, p. 677 – 681.

Lucieer, W. J., 2000. Rules of Thumb for Field and Construction Engineer in Relation to Impact. Proceedings of the 6th International Conference on the Application of Stress-wave Theory to Piles, Brazil, p. 65 – 74.

Rausche, F., Moses F., Goble G. G., 1972. Soil resistance predication from pile dynamics. *Journal of the Soil Mechanics and Foundations Division, ASCE*, **98**(SM9): 917 – 937.

Rausche, F., Goble, G. G. and Likins, G. E., 1985. Dynamic determination of pile capacity. *J. of Geotechnical Engineering, ASCE*, **111**(3): 367 – 383.

Rausche, F., 2000. Pile Driving Equipment: Capacities and Properties. Proceedings of the 6th International Conference on the Application of Stress-wave Theory to Piles, Brazil, p. 75 – 89.

Smith, E. A. L., 1960. Pile driving analysis by the wave equation. *J. Soil Mech. & Found. Eng. Div., ASCE*, **86**(4): 35 – 61.

Uto, K., Fuyuki, M. and Omor, H., 1992. New Development of Pile Driving Management System. Proceedings of the 4th International Conference on the Application of Stress-wave Theory to Piles. the Hague, p. 351 – 356.

Weele, A. F. and Schellingerhout, A. F. G., 1994. Efficient Driving of Precast Concrete Piles. Proc. Conf. Development in Geotech. Eng. Bangkok, p. 1 – 8.